Japan Journal of Research

Original Article

Application of a Disintegration-Dissolution Model to Estimate Formulation and Particle Dissolution Properties in Drug Development

Stefan Horkovics-Kovats

SHK, s.r.o., Krná 26, 985 25 Krná, Slovakia

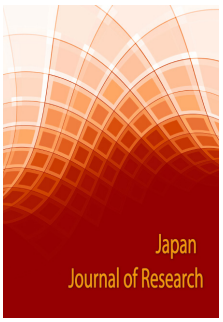

Correspondence

Stefan Horkovics-Kovats

SHK, s.r.o., Krná 26, 985 25 Krná, Slovakia

E-mail: stefan.horkovics-kovats@shk.sk

ORCID: 0000-0002-1300-4073

- Received Date: 17 Oct 2024
- Accepted Date: 23 Oct 2024
- Publication Date: 30 Oct 2024

Abstract

This systematic study investigates the minimal complexity of a first-principle-based disintegration-dissolution model (DDM) required to accurately estimate the physicochemical properties of final dosage forms (FDFs) and active pharmaceutical ingredients (APIs). Since direct measurement of API particle dissolution properties within an FDF is not feasible, simulated data sets were utilized. Dissolution time profiles were predicted for three distinct FDF compositions presented across three drug loads, considering both frequent and sparse sampling under stable and chemically degrading conditions. These predictions were then analyzed using DDMs of increasing complexity, focusing on their ability to capture critical FDF disintegration and API particle dissolution characteristics. The analysis employed nonlinear mixed-effects modeling to infer these properties.

The study demonstrates that intensive sampling significantly enhances the identification of the optimal DDM, ensuring minimal complexity while allowing reliable inference of properties. This mathematical model provides a unique opportunity to gain understanding of the dissolution properties of particles within the FDF, regardless of the API's chemical stability. By simulating and analyzing a broad range of conditions, including both non-sink and sink scenarios, the DDM offers valuable insights into how formulation disintegration, particle size distribution, and chemical degradation of the API in the medium affect the overall performance of the drug product.

The findings suggest that identifying the ideal DDM, marked by a substantial drop in objective function values, depends on selecting an appropriately complex model and utilizing intensive sampling. This approach ensures robust characterization of dissolution profiles and offers a promising method for optimizing FDF design and enhancing our understanding of drug release mechanisms at the particle level.

Keywords

Dissolution kinetics, Drug formulation, Mathematical modeling, Particle dissolution properties, SADAPT

Introduction

The bioavailability of orally administered solid drugs relies heavily on their dissolution at the site of absorption. Consequently, the dissolution properties of finished dosage forms (FDFs) are paramount for the efficacy of active pharmaceutical ingredients (APIs), formulation development, quality assurance, and in vitro–in vivo correlation (IVIVC) studies. The dissolution rate of an API released from an immediate release FDF (IR-FDF) is influenced by several factors, including the dissolution-relevant physical properties of the FDF, its disintegration characteristics, the particle size distribution (PSD) of the API, even some excipients strongly influence the dissolution properties of API [1].

The manufacturing process of oral dosage forms encompasses various steps, such as milling and drying of the API, during which the changes in the powder material can be directly measured [2,3] using methods like sieving or laser diffraction. However, processes such as direct compression and wet or dry granulation can alter the PSD of both API and excipient particles, potentially affecting the dissolution kinetics of the FDF [4]. Elevated temperatures and pressures during compaction and tableting can induce stress on API and excipient particles, leading to elastic or plastic deformation and fragmentation, depending on the structural and chemical properties of the materials involved [5]. Such changes may significantly impact FDF disintegration and dissolution [6]. As proven by chemical imaging [7], complex API structures and excipient particles may arise during these manufacturing steps. After the tableting process, the API particles are embedded in the formulation. Direct PSD measurements thereafter are not feasible.

Chemical imaging techniques have been employed to analyze the internal structure of FDFs [8-11]. These methods extract information from the scanned surfaces of FDF samples, allowing for estimation of the PSD of the drug. However, they cannot differentiate between large particles and clusters of smaller particles that form agglomerates or aggregates.

Citation: Horkovics-Kovats S. Application of a Disintegration-Dissolution Model to Estimate Formulation and Particle Dissolution Properties in Drug Development. Japan J Res. 2024;5(12):080.

If a small particle agglomerate disintegrates rapidly during the dissolution process, the observed dissolution kinetics may diverge significantly from predictions based on imaging analyses, limiting their applicability for accurate IVIVC predictions.

In our previous work, we demonstrated that the characterization of the API through its dissolution properties is sensitive to the presence of aggregates in polydisperse particle systems [12]. To analyze the disintegration of tablets, we extended our dissolution model to incorporate the FDF disintegration process, resulting in the development of the disintegration-dissolution model (DDM) [13]. The DDM was recognized as a first-principle dissolution model [14] and was initially applied to analyze routinely measured dissolution profiles of cefditoren pivoxil tablets, evaluating the effect of tableting pressure on their dissolution properties [15]. The DDM, through frequent sampling, not only identified the prolongation of disintegration time due to increased tableting pressure but also detected crystalline APIs in the formulation, independently confirmed by X-ray analysis.

Moreover, the DDM was successfully applied in the generic reformulation of ursodeoxycholic acid capsules, contributing to the understanding of the drug's pharmacokinetic behavior based on the physicochemical properties of the API and the physiological conditions in the gastrointestinal tract. The interplay between these properties formed the basis of what we term physicochemical pharmacokinetics [16]. The DDM facilitated the identification of differences at the particle lifetime distribution level, which is closely related to PSD [17] based on the dataset used to introduce the model-independent multivariate confidence region procedure [18].

Despite the successful applications of the DDM, there has yet to be a systematic investigation identifying the conditions under which DDM analysis functions optimally. This study aims to fill that gap by evaluating the impact of DDM complexity on the predictability of FDF and API particle properties derived from dissolution profiles. In addition to assessing DDM complexity, we considered various factors, including sink or non-sink states, sampling frequency, and the potential for API chemical degradation in the dissolution medium. Given that the information obtained from imaging methods regarding API characteristics can be biased, this systematic study was conducted on predicted dissolution profiles. By utilizing a first-principles-based DDM [14], we aimed to predict dissolution profiles with well-defined FDF and API particle properties, allowing for a direct comparison of estimated properties with those used for profile prediction.

Material and Methods

Structural models

A detailed description of the structural DDM can be found in [15]. Therefore, this section provides only a brief overview of the models employed in this systematic study. The models utilized N_i types of log-normally distributed particles, each with relative weights R_i, discretized into N_j parts. In each part, the particles were replaced by identical ones with expected mass calculated from the PSD.

Disintegration of the FDF was assumed to commence after a specified time lag (TLAG). The net disintegration time, DTIME, was discretized into N_k equal time steps. Consequently, during each time step, a fraction $F_k = \frac{1-exp\left(-k/N_k \times DIC\right)}{1-exp(-DIC)}$ of the dose was released into the dissolution medium, where *DIC* represents a disintegration characteristic.

For each N_i *x* N_j particle type, the k-th particle fraction was liberated from the formulation into the dissolution medium and started to dissolve at time *[LAG+(k-1)DSTEP]*. In total, this resulted in N_i *x* N_j *x* N_k differential equations each linked to the actual total amount of drug dissolved at the time *t,* $dM(t) = -\sum dm_{i,j,k}(t) - k_{deg} M(t)$, *M(t),* where k_{deg} represents the possible first-order chemical degradation rate of the API in the medium. The differential equation for the change of a drug particle at the time *t* was:

$$\frac{dm_{i,j,k}(t)}{dt} = \begin{cases} 0, & t < LAG + (k-1)DSTEP \\ -\alpha m_{i,j,k}^{2/3}\left(1 - \frac{M(t)}{c_s V}\right), & t \geq LAG + (k-1)DSTEP \end{cases}$$

where α stays for the disintegration rate.

Table 1. *Characteristics used for profile generation*

Composition	τ_1 [min] Mean (CV%)	τ_2 [min] Mean (CV%)	R_1 Mean (CV%)	σ_1 [min] Mean (CV%)	σ_2 [min] Mean (CV%)	DISINT [min] Mean (CV%)	TLAG [min] Mean (CV%)	L=0.15 [mg] Mean (CV%)	L=0.50 [mg] Mean (CV%)	L=0.85 [mg] Mean (CV%)
1	2.06 (4.38)	9.97 (5.19)	0.80 (4.87)	1.93 (5.56)	3.97 (3.30)	15.35 (12.35)	1.55 (12.03)	0.152 (1.79)	0.504 (2.58)	0.852 (2.31)
2	4.07 (3.17)	20.19 (5.58)	0.49 (6.04)	1.99 (5.49)	1.97 (4.75)	10.06 (16.83)	1.11 (13.08)	0.149 (2.24)	0.495 (1.98)	0.851 (1.82)
3	8.04 (3.81)	40.01 (6.54)	0.30 (6.13)	3.03 (4.60)	1.53 (4.35)	5.03 (16.90)	0.43 (13.86)	0.148 (1.77)	0.503 (2.37)	0.854 (1.62)

Legend: τ_1 and τ_2 represent the mean lifetime of the first and second particle population, respectively. R_1 denotes the relative weight of the first particle population. σ_1 and σ2 indicate the standard deviation of the log/linear lifetime distributions. DISINT refers to the time measured until the total disintegration of the FDF, while TLAG represents the time before disintegration begins. The values represent the means and coefficinets of variation CVs (%) of the parameters used accross 10 simulations for varying average drug loads of 0.15, 0.50, and 0.85, respectively, across a total of 9 different FDF models.

Prediction of dissolution profiles

The saturation concentration, c_s, of the arbitrary drug was set to 1 mg/mL, and dissolution was assumed to occur in volume, V, of 1000 mL of liquid, with the chemical degradation rate, k_{deg}, set to null or 0.0578 min^{-1} (half-life of 12 minutes). The parameters used for profile prediction are summarized in Table 1. To reduce the number of evaluated parameters, the particle lifetime, defined as the minimal time needed to dissolve a particle of initial mass m_0 in an infinite volume under given hydrodynamic conditions, was as expressed as $\tau = \frac{3m_0^{\gamma_3}}{\alpha}$ and evaluated as a summary characteristic of the particle.

The prediction of dissolution profiles was achieved by numerical integration of model DDM0 (see Table 2) using RK4 method of Berkely Madonna, software version 10.4.2. For each composition and drug load $L = \frac{Dose}{c_s V}$, ten individual profiles were predicted, and to the predicted profiles a normally distributed random error function was added, to mimic measurement errors of real data. From the obtained data sets, subsets representing intensive or sparse sampling were created. The analysis was based on three compositions, three drug loads, two sampling schemes, with or without considering API chemical degradation in the dissolution medium. The FDF disintegration- and API particle dissolution characteristics were estimated from the data sets with DDMs models listed in Table 2. This resulted in 216 model evaluations. Each composition/drug load data set of ten profiles was analyzed separately, to exclude the influence of other composition/drug load data on the determined characteristics.

Between curve variability

The applied population modeling simultaneously estimated the population mean and between curve variability parameters. All parameters were assumed to be log-normally distributed except for the estimated fractions that were modeled by a logistics transformation described previously [19]. An additive and a proportional residual error model was used in the analysis.

DDM parameter estimation

The model parameters were estimated using the importance sampling algorithm (pmethod = 4 in S-ADAPT software, version 1.57) by minimizing (-1 x log-likelihood in S-ADAPT) as objective function. SADAPT-TRAN (19) was used for model design and evaluation of results [20,21].

Table 2. *Structure of disintegration-dissolution models*

Utilization	DDM	N_i	N_j	N	N_p
Data generation	DDM0	2	7	211	
Data analysis	DDM1	1	1	16	4
	DDM2	1	3	46	5
	DDM3	2	1	31	6
	DDM4	2	3	91	8
	DDM5	3	1	46	8
	DDM6	3	3	136	11

Legend: *the net disintegration time (DTIME), calculated as the difference between the total disintegration time (DISINT) and the lag time (TLAG), was divided into N_k =15 equal time intervals in all models. For the given DDM model, N_i represents the number of particle populations, each discretized into N_j sub-populations, defining N differential equations withing the model. N_p indicates the number of population means in the model.*

Comparison of dissolution profiles

Dissolution profiles were compared using the similarity factor *F2* [22]. In the data set with no chemical degradation, the first mean value of dissolution was considered where the CV% was below 20%, and last considered data point was the first value > 85%. In case of API chemical degradation, the first mean value of dissolution was considered where CV% was below 20%, one after the maximal dissolution value was considered as last value for the calculation of *F2*.

Results

Prediction of in silico dissolution time profiles and their comparison

Using the disintegration-dissolution model, DDM0, specified in Table 2, dissolution profiles of three compositions at three drug loads, L = 0.15, 0.50 and 0.85, respectively, were predicted, Figure 1.The parameters used for prediction are summarized in Table 1. To each composition/drug-load combination ten dissolution profiles with slightly different parameter settings were predicted, for *F2* statistics the mean values were taken.

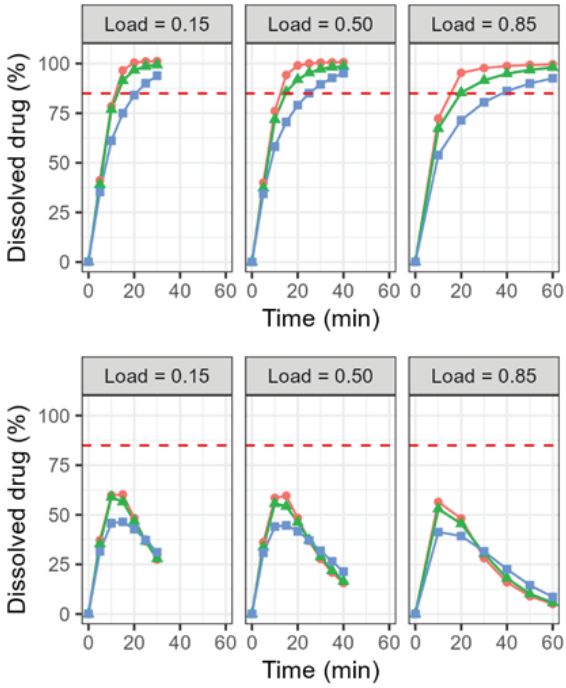

Figure 1. *Generated dissolution profiles*

Generated mean dissolution profiles of three compositions showing the sparse sampling results. Upper section shows results for a stable API, while the lower section shows results for a chemically unstable API in the dissolution medium. Composition 1, 2, and 3 (defined in Table 1) are represented with red circles, green triangles, and blue squares, respectively. Drug loads of 0.15, 0.5, and 0.85 are indicated above the corresponding profiles. The dotted line markes the of 85% dissolution level, after which only one measurement point was used for F2 calculation with stable API. Sampling time increased with higher drug loads to ensure at least three data points below the 85% dissolution level for the stable drug.

The higher drug load reduced the apparent dissolution kinetic of the API from FDF, as shown in Figure 1. This change in dissolution kinetics was reflected by the increased separation of the dissolution profiles affecting the *F2* values, see Table 3. The comparison of compositions 1 and 2 showed similar profiles (*F2* > 50) for cases with and without degrading API. The comparison of compositions 2 and 3 indicated missing similarity (*F2* < 50) at stable API conditions; however, at degrading conditions the profiles were similar as all *F2* values were above 50. The most marked differences were observed between the compositions 1 and 3, where under all conditions, no similarity of the profiles was found.

Identification of DDM model for analysis

The individually predicted release profiles were subjected to the analysis employing mechanistic models of increasing complexity. DDM1, DDM3 and DDM5 considered 1, 2 or 3 discrete particle populations, while DDM2, DDM4 and DDM6 considered log/normal distributions of particles within the formulations.

The obtained average objective function values were compared for the tested structural models and are summarized in Figure 2. The models employing intensively sampled data sets show markedly higher sensitivity to the complexity of the structural models. In general, a drop in the objective functions of the optimization is observed for DDM3 when employing intensive sampling. This observation was repeated in case of unstable API, part B of Figure 2.

Only the results obtained from DDM3 are reported here, as the more complex structural models utilized a much higher number of differential equations, leading to substantially longer optimization time without additional benefit for parameter determination.

Assessment of FDF characteristics

The dose of API, lag-time of the disintegration process, and time of finishing the formulation disintegration were assessed from the predicted dissolution profiles, utilizing data sets of sparse and intensive sampling for stable and chemically degrading drug in the dissolution medium. The results for chemically stable API are shown in Figure 3, while the results for chemically degrading API are given in Supplementary materials. The best assessed FDF characteristic is the dose of formulation, which could be determined under all drug-load and sampling conditions independently of the stability properties of the API.

The lag-time of the disintegration process can only be precisely determined under intensive sampling. Obviously, the lack of data points at the beginning of the disintegration process influenced greatly the determinability of the lag-time. Similarly, the disintegration time is better assessed under intensive sampling conditions. Under these conditions, the FDF characteristics could be determined, for all drug-loads, independent of the stability properties of the API.

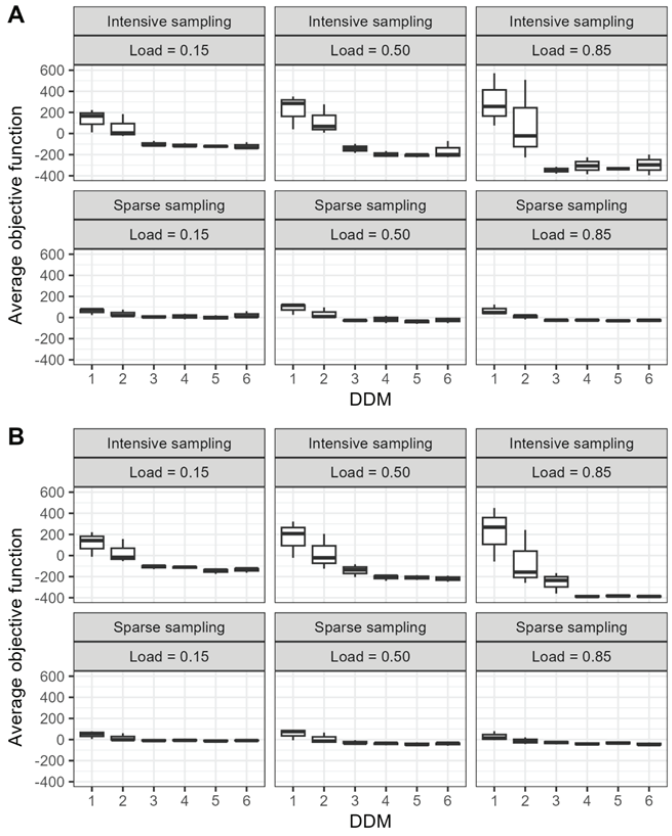

Figure 2. *Average objective functions*
Average objective function values under the investigated settings as a function of disintegration-dissolution model complexity. Panel A represents results for a chemically stable API, while Panel B shows results for a chemically unstable API.

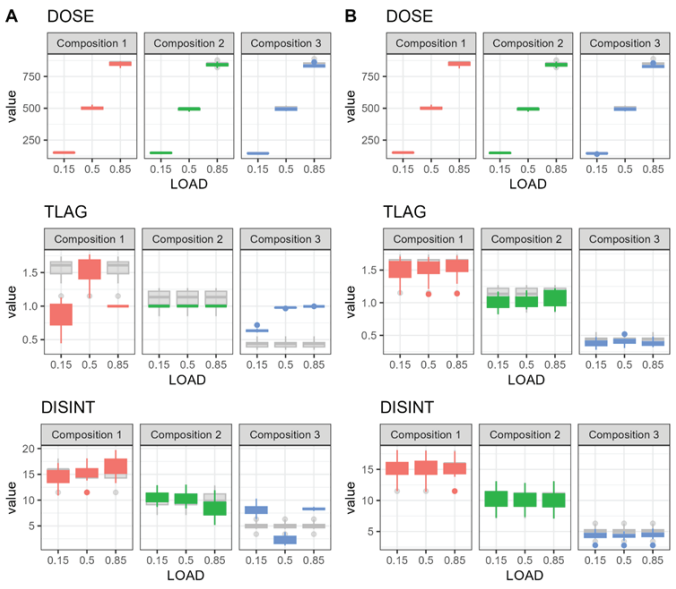

Figure 3. FDF characteristics

Characteristics of the FDF assessed from generated dissolution profiles under stable API conditions, analyzed with the DDM3 model with sparse (A) and intensive (B) sampling. The characteristics for compositions 1 (red), 2 (green), and 3 (blue) are shown alongside the values used for the generation of the dissolution profiles (gray). Parameters include DOSE – the dose in the formulation, TLAG – lag time before disintegration begins, and DISINT – the total disintegration time from the start of the experiment until disintegration completion.

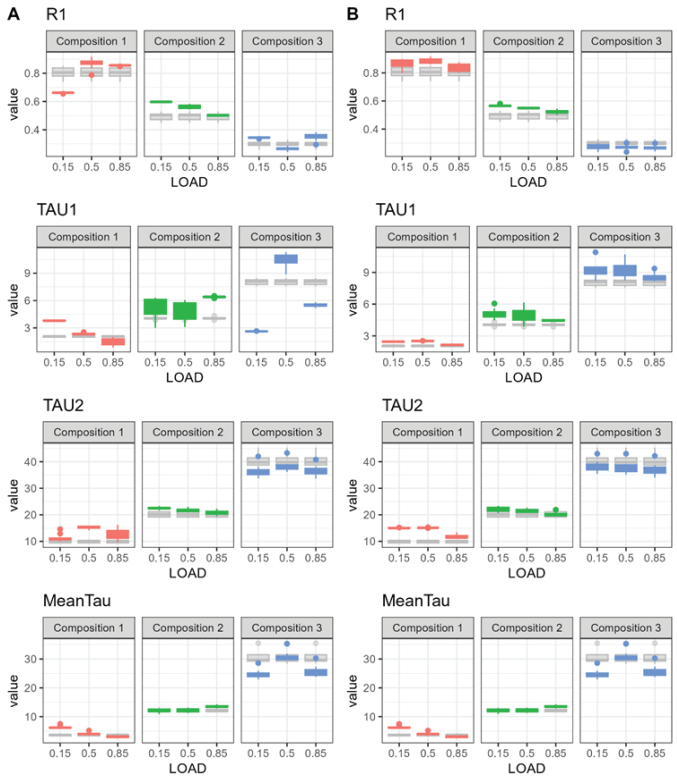

Figure 4. *API characteristics*

Characteristics of API particles assessed from the generated profiles under stable API conditions, analyzed using the DDM3 model with sparse (A) and intensive (B) sampling. The characteristics for compositions 1 (red), 2 (green), and 3 (blue) are shown alongside the values used for generating the dissolution profiles (gray). R1 – relative weight of the particles with shorter lifetime, TAU1 – the lifetime of first type of particles, TAU2 – the lifetime of the second type of particles, MeanTau – weighted average of particles lifetime in the formulation.

Assessment of API particle characteristics

From the dissolution profiles the relative weights of the first sub-populations, R_1, lifetime for the first, τ_1, and second, τ_2, sub-populations of various drug-loads for stable and chemically degrading drug employing sparse- and intensive sampling, were determined. The results are summarized in Figure 4, while the results for chemically degrading API are given in Supplementary materials. The data shows that the three parameters are not totally independent. In case the relative weight of the first population in a formulation is underestimated, (e.g., sparse sampling of stable API, drug load of formulation = 0.15), the remaining parameters are balanced in a way that the weighted mean of the lifetimes, matched the values calculated from the values used for profile simulation. The intensive sampling reduces the variability of the weighted lifetimes determined from the assessed values of R_1, $\tau_1$and τ_2. The chemical degradation of the API, especially under sparse sampling, influenced the assessment of the lifetime τ_1. This phenomenon can be explained by the low relative weight of that sub-population in the sample and the uncertainty of the determined lag-time and disintegration time.

Discussion

The aim of the presented systematic study was to identify the minimal complexity of a DDM that could correctly extract the dissolution relevant FDF and API properties. The dissolution time profiles were measured with different settings. Due to the lack of suitable pharmaceutical forms with precisely defined API particle properties, the investigation was performed on predicted data sets. The available physical measurements, mostly spectroscopic methods [8-11], provided an indirect information based on the density of a particular signal from the surface of the formulation. From such assessment of the particle size, the agglomerates/aggregates signals cannot be distinguished from signals of large particles. This possibly may lead to a biased assessment of the dissolution behavior. Even the characterization of the initial powder is challenging, as the laser diffraction technique does not distinguish between scattering by single particles or by clusters of particles forming an agglomerate or an aggregate. For non-spherical particles, an equivalent-sphere size distribution is obtained because the technique uses the assumption of spherical particles in its optical model. The resulting PSD may be different from those obtained by methods based on other physical principles (such as sedimentation or sieving) [2].

On top of that, the tableting process can cause plastic deformation and/or crash the API particles with a concomitant change in the shape of the particles. The changed shape [23,24] and hence the changed relative surface of dissolving particles influences the particle dissolution kinetics [12,25]. For these reasons, the lifetime of particles, i.e., a summary characteristic defined as the time needed for the particle to dissolve completely in infinite volume of medium under the given hydrodynamic conditions, was introduced [13]. For the lifetime calculation of a particle, an assumption of its shape is not necessary.

The study considered three compositions, characterized by increasing particle sizes expressed in the halftimes τ_1 and τ_2. The relative weight of smaller particles in the formulation decreased as the overall halftime of particles increased. This together with shortening the disintegration time of the formulations, see Table 1, aimed to make the dissolution profiles more similar, and hence it posed a challenge to DDM analysis in identifying the differences between the formulations. Despite the similarity of dissolution profiles between composition 1 and 2 assessed by factor *F2*, the formulations were characterized with different disintegration times. The observed dissolution profiles are then an interplay between the disintegration kinetics and the API particle dissolution properties, which could influence the bioavailability of a drug in case of narrow absorption window in the GI tract and/or considerable chemical degradation of the drug in the stomach. In such cases, formulation development decisions should be based both on dissolution profile analysis and disintegration analysis. Hence, to use only the disintegration testing could be insufficient [26].

The increase of drug load leading to dissolution conditions beyond sink conditions affected the profiles. As shown in Figure 1, the differences under conditions of stable API were more pronounced with increasing drug load. This fact was reflected in *F2* evaluation (22) (Table 3), where the similarity factor *F2* for comparison composition 1 vs composition 2, and composition 1 vs composition 3 decreased with increasing drug load. The sampling frequency for *F2* statistics showed an impact on the *F2* values. When a chemically degrading API was modelled, the *F2* statistics identified only compositions 1 and 3 as non-similar, see Table 3.

Table 3. *Comparison of generated dissolution profiles*

Drug load	*Degradation*	*sampling*	*Sampling used for F2 calculation*	*F2 (12)*	*F2 (23)*	*F2 (13)*
0.15	absent	intensive	Every minute from 3 to 13	82.47	45.93	44.10
0.50			Every minute from 3 to 13	66.72	48.54	41.13
0.85			Every minute from 3 to 14	62.14	48.83	39.75
0.15		sparse	3, 7, 12 minutes	80.82	44.25	43.92
0.50			3, 8, 13 minutes	66.72	46.23	41.13
0.85			3, 8, 14 minutes	63.93	48.17	39.87
0.15	present	intensive	Every minute from 3	85.44	50.30	47.48
0.50			Every minute from 3	74.09	52.41	46.21
0.85			Every minute from 3	71.22	51.93	44.89
0.15		sparse	4, 8, 12, 16 minutes	78.82	50.97	46.76
0.50			3, 8, 13. 18 minutes	73.29	54.52	47.60
0.85			3, 8, 13, 18 minutes	69.82	53.74	45.58

Legend: the F2 (xy) indicates the similarity factor between the compositions x and y. Sampling was conducted up to 30, 40, and 60 minutes for drug load of 0.15, 0.5, and 0.85, respectively.

The analysis of the generated dissolution profiles with models indicated in Table 1 led to substantial lowering of the objective function as the complexity of the model increased. A major drop in the objective function values (Figure 2) could be observed using DDM3 at intensive sampling independent of the chemical stability of API, while the increased drug load of the system has a positive influence on DDM identification.

This model correctly implemented two kinds of particles in the formulations, yet the distribution of these particles was not accounted for. The inclusion of log/linear particle lifetime distribution into DDM4 did not have a significant impact on the determination of the model parameters. Nonetheless, likelihood ratio tests showed that the fitting was notably improved with the addition of the particle distribution (data not shown). In accordance with William Ockham's razor, we have opted for DDM3. This way we reduced the number of differential equations and the time needed for optimization. It should be noted that the marked drop in the objection function can be observed only in case of intensive sampling, strongly advocating the analysis of dissolution profiles using intensive sampling and beyond sink conditions. A sparse sampling study could be performed with over simplified mechanical models, leading to biased estimation of FDF and API particle properties.

The evaluation of more complex three particle population models (DDM5 and DDM6) made the creation of the weighted average τ value necessary, as in such cases a direct comparison of the identified lifetimes to the model parameters used for the profile prediction would not be possible.

The DDM-based analysis of the profiles demonstrated that this method remains applicable even when the API is chemically unstable during the dissolution measurement. This capability highlights a significant advantage of the DDM, as it is sensitive to differences in formulations even under such challenging conditions.

Contrary to *F2* statistics or model-dependent or independent multivariate distance tests [18,27-29]. DDM does not evaluate the similarity of the profiles, but rather identifies the difference in the disintegration characteristics of the formulation, Figure 3, and the characteristics of the API particles in the formulation, Figure 4.

The estimation of the disintegration characteristics is of special importance as some limitations in developing direct techniques for evaluating disintegration profiles are linked to drawbacks in the disintegration testing apparatus and lack of theoretical models [30]. The disintegration testing itself causes additional mechanical stress and changes the hydrodynamic conditions during the measurements [31]. The increased mechanical stress during the disintegration measurement [32] influences the disintegration process and the dissolution time profile of formulation. The influence of the FDF disintegration on the FDF dissolution was extensively discussed in our previous research [13,15].

Analysis of dissolution time profiles utilizing first-principle structural models enables formulation characterization based on key properties influencing dissolution time profiles of a formulation. Such a method has enormous potential for IVIVC model applications, as well for oral formulation optimization [16]. The integration of DDM into formulation development could further enhance the analysis of dissolution profiles, ultimately benefiting pharmaceutical development.

Conclusions

This systematic study underscores the utility of a first-principle-based DDM in accurately estimating the physicochemical properties of FDFs and APIs. The findings suggest that DDM can serve as a robust tool for understanding the dissolution kinetics of drug formulations, even in cases where the API is chemically unstable during dissolution experiments.

The ability of DDM to provide insights into the disintegration and dissolution properties of particles within FDFs has significant implications for clinical practice. For instance, this model could enhance the formulation development process, leading to optimized drug products with improved bioavailability. By facilitating the characterization of dissolution profiles under various conditions, DDM can aid in the design of more effective therapies tailored to individual patient needs.

In conclusion, integrating DDM into routine formulation practices not only fosters innovation in drug development but also aligns with the goals of personalized medicine and improved therapeutic outcomes for patients.

Acknowledgments

The author thanks Mrs. Pushpa Balasubramanian for proofreading the manuscript. Part of the research results was obtained using the computational resources procured in the national project National competence centre for high performance computing (project code: 311070AKF2) funded by European Regional Development Fund, EU Structural Funds Informatization of society, Operational Program Integrated Infrastructure.

Conflict of interest

No funding was provided for this research, so there is no conflict of interest.

References

1. Strickley RG. Solubilizing excipients in oral and injectable formulations. Pharm Res. 2004;21(2):201-230. doi:10.1023/b:pham.0000016235.32639.23
2. USP<429> [Internet]. [cited 2022 Nov 10]. Available from: https://www.usp.org/sites/default/files/usp/document/harmonization/gen-chapter/g13_pf_35_3_2009.pdf
3. USP<786> [Internet]. [cited 2022 Nov 10]. Available from: https://www.usp.org/sites/default/files/usp/document/harmonization/excipients/harmonization-april-2022-m99584.pdf
4. Sun Z, Ya N, Adams RC, Fang FS. Particle size specifications for solid oral dosage forms: A regulatory perspective. Am Pharm Rev. 2010;13(4):68–73.
5. Chattoraj S, Sun CC. Crystal and particle engineering strategies for improving powder compression and flow properties to enable continuous tablet manufacturing by direct compression. J Pharm Sci. 2018;107(4):968–74.
6. Haruna F, Apeji YE, Oparaeche C, Oyi AR, Gamlen M. Compaction and tableting properties of composite particles of microcrystalline cellulose and crospovidone engineered for direct compression. Futur J Pharm Sci. 2020;6(1). doi: 10.1186/s43094-020-00055-9
7. Sacré PY, De Bleye C, Chavez PF, Netchacovitch L, Hubert P, Ziemons E. Data processing of vibrational chemical imaging for pharmaceutical applications. J Pharm Biomed Anal. 2014;101:123-140. doi:10.1016/j.jpba.2014.04.012.
8. Kuriyama A, Ozaki Y. Assessment of active pharmaceutical ingredient particle size in tablets by Raman chemical imaging validated using polystyrene microsphere size standards. AAPS PharmSciTech. 2014;15(2):375-387. doi:10.1208/s12249-013-0064-9.
9. Gowen AA, O'Donnell CP, Cullen PJ, Bell SEJ. Recent applications of chemical imaging to pharmaceutical process monitoring and quality control. Eur J Pharm Biopharm. 2008;69:10–22. doi: 10.1016/j.ejpb.2007.10.013
10. Gamble JF, Tobyn M, Hamey R. Application of image-based particle size and shape characterization systems in the development of small molecule pharmaceuticals. J Pharm Sci. 2015;104:1563–74. doi: 10.1002/jps.24382
11. O'Neil A, Edwards H. Spectroscopic characterization. In: Solid state characterization of pharmaceuticals [Internet]. Wiley; 2011. p. 71–134. Available from: https://onlinelibrary.wiley.com/doi/10.1002/9780470656792.ch3
12. Horkovics-Kovats S. Characterization of an active pharmaceutical ingredient by its dissolution properties: amoxicillin trihydrate as a model drug. Chemotherapy. 2004;50(5):234-244. doi:10.1159/000081944.
13. Horkovics-Kovats S. Disintegration rate and properties of active pharmaceutical ingredient particles as determined from the dissolution time profile of a pharmaceutical formulation: an inverse problem. J Pharm Sci. 2014;103(2):456-464. doi:10.1002/jps.23767.
14. Zaborenko N, Shi Z, Corredor CC, et al. First-Principles and Empirical Approaches to Predicting In Vitro Dissolution for Pharmaceutical Formulation and Process Development and for Product Release Testing. AAPS J. 2019;21(3):32. Published 2019 Feb 21. doi:10.1208/s12248-019-0297-y.
15. Horkovics-Kovats S, Brunovský P, Pichler A, Bulitta JB. Population data analysis of dissolution time profiles: Assessment of physicochemical properties of the drug, drug particles and the pharmaceutical formulation. Eur J Pharm Sci. 2015;78:245-254. doi:10.1016/j.ejps.2015.07.017.
16. Horkovics-Kovats S, Ulč I, Vít L, Němec B, Rada V. Physicochemical pharmacokinetics as an optimization tool for generic development: A case study. Eur J Pharm Sci. 2018;111:349-357. doi:10.1016/j.ejps.2017.10.018
17. Horkovics-Kovats S. Comparison of dissolution time profiles: No similarity but where is the difference? Eur J Pharm Sci. 2018;121:9–15. doi: 10.1016/j.ejps.2018.05.017
18. Tsong Y, Hammerstrom T, Sathe P, Shah VP. Statistical assessment of mean differences between two dissolution data sets. Drug Inf J. 1996;30:1105–12. doi: 10.1177/009286159603000427
19. Bulitta JB, Bingölbali A, Shin BS, Landersdorfer CB. Development of a new pre- and post-processing tool (SADAPT-TRAN) for nonlinear mixed-effects modeling in S-ADAPT. AAPS J. 2011;13(2):201-11. doi: 10.1208/s12248-011-9257-x.
20. Bauer RJ, Guzy S, Ng C. A survey of population analysis methods and software for complex pharmacokinetic and pharmacodynamic models with examples. AAPS J. 2007;9(1):E60-E83. doi:10.1208/aapsj0901007
21. Bulitta JB, Landersdorfer CB. Performance and robustness of the Monte Carlo importance sampling algorithm using parallelized S-ADAPT for basic and complex mechanistic models. AAPS J. 2011;13(2):212-226. doi:10.1208/s12248-011-9258-9
22. Moore JW, Planner HH. Mathematical comparison of dissolution profiles. Pharm Technol. 1996;20:65–74.
23. Heng JY, Thielmann F, Williams DR. The effects of milling on the surface properties of form I paracetamol crystals. Pharm Res. 2006;23(8):1918-1927. doi:10.1007/s11095-006-9042-1.
24. Ho R, Naderi M, Heng JY, et al. Effect of milling on particle shape and surface energy heterogeneity of needle-shaped crystals. Pharm Res. 2012;29(10):2806-2816. doi:10.1007/s11095-012-0842-1.
25. Horkovics-Kovats S. Dissolution and coarsening of polydisperse, polymorph drug particles liberated from a disintegrating finished dosage form: Theoretical considerations. Eur J Pharm Sci. 2016;91:265-277. doi:10.1016/j.ejps.2016.05.003.
26. EMA. ICH topic Q 6 A specifications: Test procedures and acceptance criteria for new drug substances and new drug products: Chemical substances step 5 note for guidance specifications: Test procedures and acceptance criteria for new drug substances and new drug products: Chemical substances [Internet]. 2000. Available from: http://www.emea.eu.int
27. Sathe PM, Tsong Y, Shah VP. In-vitro dissolution profile comparison: statistics and analysis, model dependent approach. Pharm Res. 1996;13(12):1799-1803. doi:10.1023/a:1016020822093.
28. Wang Y, Snee RD, Keyvan G, Muzzio FJ. Statistical comparison of dissolution profiles. Drug Dev Ind Pharm. 2016;42(5):796-807. doi:10.3109/03639045.2015.1078349.
29. Hoffelder T, Gössl R, Wellek S. Multivariate equivalence tests for use in pharmaceutical development. J Biopharm Stat. 2015;25(3):417-437. doi:10.1080/10543406.2014.920344.

30. Jange CG, Wassgren CR, Ambrose K. The Significance of Tablet Internal Structure on Disintegration and Dissolution of Immediate-Release Formulas: A Review. Powders. 2023; 2(1):99-123. doi. 10.3390/powders2010008
31. Almukainzi M, Salehi M, Araci Bou-Chacra N, Löbenberg R. Investigation of the performance of the disintegration test for dietary supplements. AAPS J. 2010 Dec;12(4):602-7. doi: 10.1208/s12248-010-9221-1.
32. Garbacz G, Klein S, Weitschies W. A biorelevant dissolution stress test device - background and experiences. Expert Opin Drug Deliv. 2010;7(11):1251-1261. doi:10.1517/17425247.2010 .527943.

Supplementary Materials

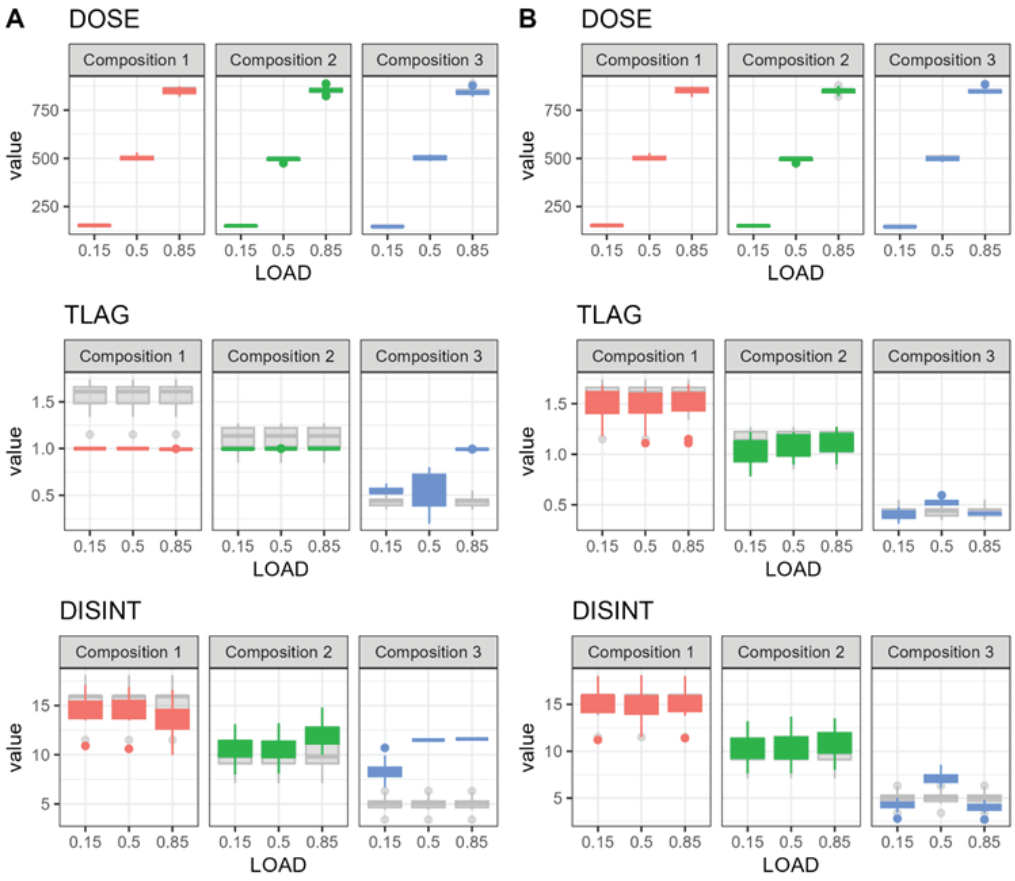

Figure A. *FDF characteristics*

Characteristics of FDF assessed from the generated profiles under conditions of chemically unstable API, analyzed with the DDM3 model employing sparse (A) and intensive (B), respectively. The characteristics of composition 1 (red), 2 (green) and 3 (blue), respectively, are shown together with the values used for the generation of the dissolution profiles (gray). DOSE – dose in the formulation, TLAG – lag time before starting the disintegration process, DISINT – time from beginning of experiment until the end of the disintegration process.

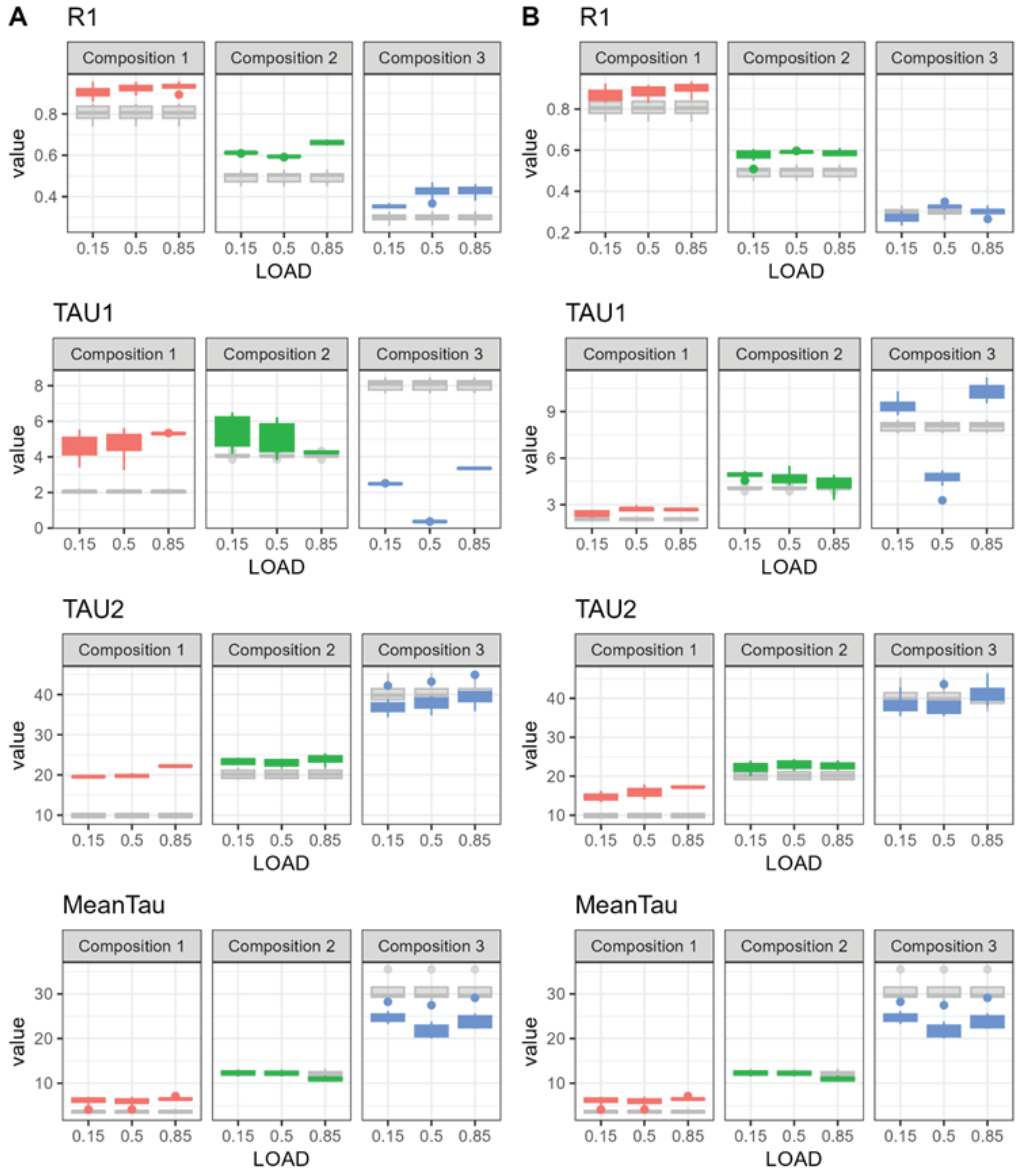

Figure B. *API characteristics*

Characteristics of API particles assessed from the generated profiles under conditions of chemically unstable API, analyzed with the DDM3 model employing sparse (A) and intensive (B), respectively. The characteristics of composition 1 (red), 2 (green) and 3 (blue), respectively, are shown together with the values used for the generation of the dissolution profiles (gray). R_1 *– relative weight of the particles with shorter lifetime, TAU1 – lifetime of first kind of particles, TAU2 – lifetime of the second kind of particles, Mean Tau – weighted average of particles lifetime in the formulation.*